

Energy-maximising tracking control for a nonlinear heaving point absorber system commanded by second order sliding modes

Mosquera, F. D.* Faedo, N.** Evangelista, C. A.*
Puleston, P. F.* Ringwood, J. V.***

* *Instituto LEICI, Facultad de Ingeniería UNLP - CONICET, Argentina (e-mail: facundo.mosquera@ing.unlp.edu.ar).*

** *Marine Offshore Renewable Energy Lab., Department of Mechanical and Aerospace Engineering, Politecnico di Torino, Italy.*

*** *Centre for Ocean Energy Research, Department of Electronic Engineering, Maynooth University, Ireland.*

Abstract: Energy-maximising control has proven to be of fundamental aid in the pathway towards commercialisation of wave energy conversion technology. The WEC control problem is based upon the design of a suitable control law capable of maximising energy extraction from the wave resource, while effectively minimising any risk of component damage. A particularly well-established family of WEC controllers is based upon a composite structure, where an optimal velocity reference is generated via direct optimal control procedures, followed by a suitable tracking control strategy. This paper presents the design and synthesis of a second order sliding mode controller to attain a reference tracking for a wave energy system. The presented approach can inherently handle parameter uncertainty in the model, which is ubiquitous within hydrodynamic modelling procedures. Furthermore, the proposed sliding mode controller has relatively mild computational requirements, and finite-time convergence to the designed surface, hence being an ideal candidate for real-time energy-maximising control of WEC systems.

Copyright © 2022 The Authors. This is an open access article under the CC BY-NC-ND license (<https://creativecommons.org/licenses/by-nc-nd/4.0/>)

Keywords: Wave energy, Optimal control, Sliding mode control, Super twisting

1. INTRODUCTION

Successful commercialisation of wave energy conversion (WEC) systems is inherently linked to the availability of control technology, capable of lowering the associated levelised cost of energy (LCoE) via maximisation of the energy absorbed by the device from the incoming wave field (Korde and Ringwood, 2016; Ringwood, 2020). Such an objective is commonly formalised in terms of an appropriate optimal control problem (OCP), which attempts to increase the capabilities of the WEC device in terms of energy performance, via its corresponding power take-off (PTO) actuator system, while consistently guaranteeing satisfaction of physical limitations (Faedo et al., 2020a).

A variety of direct optimal control methods found their way into the wave energy field, aiming to provide consistent numerical solutions to the associated OCP, ranging from relatively standard techniques, such as model predictive control (Hals et al., 2011), to families of tailored discretisations (see e.g. Bacelli and Ringwood (2014); Herber and Allison (2013); Li (2017); Genest and Ringwood (2016); Faedo et al. (2021a)). Within these latter fami-

lies of methods, strategies capable of providing efficient solutions to the WEC OCP can be found, guaranteeing a well-posed solution, even under consideration of nonlinear WEC dynamics, while exhibiting low computational requirements.

Though effectively capable of producing an optimal law, virtually all direct optimal control-based methods are implemented based on a two-level control architecture (see e.g. Faedo et al. (2017); Genest and Ringwood (2016)), as schematically depicted in Fig. 1. In particular, the outer loop acts as a ‘trajectory generator’, typically providing an optimal energy-maximising velocity profile on a regular time interval, based upon an estimate of the so-called wave excitation (*i.e.* the force exerted on the device due to the incoming wave field), while the inner loop is in charge of effectively tracking the computed reference in real-time¹. Given the inherent complexity behind hydrodynamic WEC modelling, the presence of uncertainty within control-oriented models is effectively ubiquitous, specifically with respect to certain physical parameters (Giorgi et al., 2020). As such, robust control strategies, capable of guaranteeing consistent tracking of the computed optimal motion profile, are crucial within the inner level of the corresponding control architecture, being hence able to

* This research was supported by the Facultad de Ingeniería, Universidad Nacional de La Plata (UNLP), CONICET and Agencia I+D+i, from Argentina.

This project has received funding from the European Union’s Horizon 2020 research and innovation programme under the Marie Skłodowska-Curie grant agreement No 101024372.

¹ This resembles the wind energy case, where a rotational velocity setpoint is determined from incident wind speed, optimal tip/speed ratio, and blade pitch (see e.g. (Ringwood and Simani, 2015))

secure optimal energy absorption performance, even in the presence of (potentially significant) modelling uncertainty.

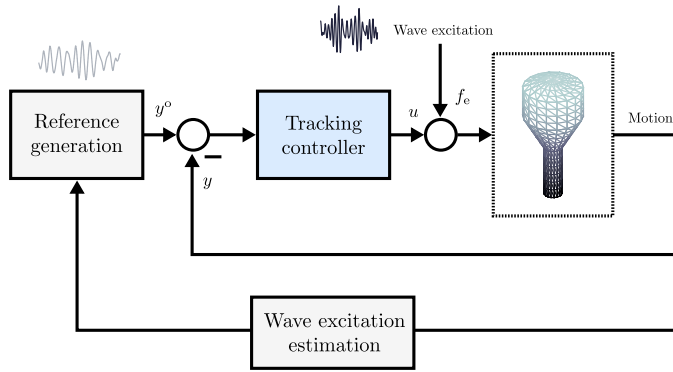


Fig. 1. Typical two-level WEC control architecture.

Motivated by the inherent requirement of robust tracking control strategies to successfully implement energy-maximisation, others authors utilised sliding mode control (SMC) to track an optimal reference in the inner loop (Wahyudie et al., 2013; Zhang and Li, 2020), obtaining promising results. Nevertheless, classical first order SMC may give rise to chattering, an undesired phenomenon characterised by finite-frequency and finite-amplitude oscillations, due to the use of a discontinuous control action applied to the first time derivative of the sliding variable (Utkin and Lee, 2006), and particularly undesirable in mechanical systems.

To reduce chattering, several innovative solutions have been proposed over the years, with second order sliding mode (SOSM) control one of the most widespread and successful approaches (Levant, 1993; Bartolini et al., 1999; Shtessel et al., 2013). In general terms, the discontinuous action in SOSM techniques acts on the second time derivative of the sliding variable, providing a smoother control signal than that obtained via first order SMC. Such control action represents a significant advantage to the lifespan of system actuators (Shtessel et al., 2013). In this paper, we utilise a Super-Twisting (ST) algorithm, to accomplish the objective proposed robustly and with finite time convergence to the optimal velocity profile given from the outer loop.

Generation of the optimal reference (velocity) profile, in the outer loop, is performed via the so-called moment-based approach (Faedo et al., 2021a), incorporating both the corresponding nonlinear WEC dynamics, and a nonlinear PTO efficiency function, describing the mechanical-to-electrical conversion stage. With the same model, the gains of the ST algorithm are calculated to guarantee finite time convergence to the velocity reference and robust permanence of the trajectories of the system at the optimal operation point, while dealing with hydrodynamic uncertainty and perturbations.

The remainder of this paper is organised as follows. Section 2 presents the particular point absorber device considered as a case study, while Section 3 describes the adopted optimal reference generation strategy. Section 4 presents, and describes, the design of the proposed SOSM control algorithm for reference tracking, while Section 5 provides a numerical appraisal of the performance obtained with the

proposed SOSM strategy. Finally, Section 6 summarises the main conclusions of our study.

2. CONTROL-ORIENTED WEC DYNAMICS

The device considered throughout our paper is essentially a heaving point absorber system, schematically illustrated in Fig. 2, and inspired by that originally described in (Hals et al., 2016). If we constrain the WEC system to move in heave, the equation of motion can be written in terms of a finite-dimensional system Σ given, for $t \in \mathbb{R}^+$, by the following set of equations²

$$\Sigma : \begin{cases} \dot{x} = f(x, \zeta) = Ax + B\zeta + g(x), \\ y = h(x) = Cx, \end{cases} \quad (1)$$

where the associated state-vector is $x = [z \dot{z} \Gamma^T]^T$, $x(t) \in \mathbb{R}^n$, $n = 2 + n_r$, with $t \mapsto z(t) \in \mathbb{R}$ the displacement of the WEC system, and $t \mapsto \Gamma(t) \in \mathbb{R}^{n_r}$ the state-vector describing the fluid memory effects acting on the device, *i.e.* we define the so-called radiation force in terms of a linear, continuous-time, strictly proper, finite-dimensional³ system, written as

$$\Sigma_r : \begin{cases} \dot{\Gamma} = F\Gamma + Gy, \\ f_{\text{rad}} = H\Gamma, \end{cases} \quad (2)$$

with $F \in \mathbb{R}^{n_r \times n_r}$, $\lambda(F) \subset \mathbb{C}_{<0}$, and $(G, H^T) \in \mathbb{R}^{n_r} \times \mathbb{R}^{n_r}$.

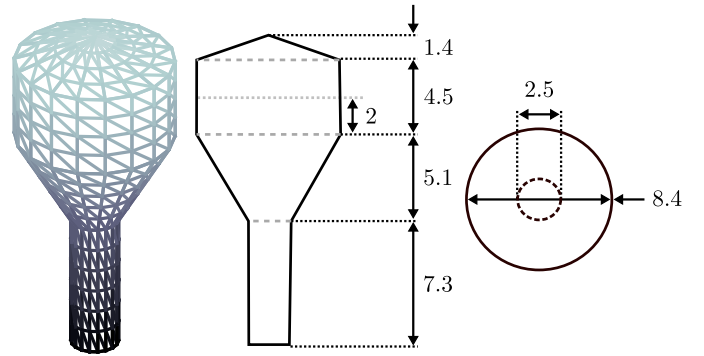


Fig. 2. Schematic illustration of the point absorber WEC device. Dimensions are in metres.

The map $\zeta = f_e - u$ represents the total input force, where $t \mapsto f_e(t) \in \mathbb{R}$ is the external (uncontrollable) force exerted by the waves on the hull of the WEC system, *i.e.* the wave excitation force, while $t \mapsto u(t) \in \mathbb{R}$ denotes the (user-supplied) control law, to be optimally designed such that wave energy extraction is effectively maximised. The triple $(A, B, C^T) \in \mathbb{R}^{n \times n} \times \mathbb{R}^n \times \mathbb{R}^n$ in (1) is defined by

$$A = \begin{bmatrix} A^0 & -B^0 H \\ GC^0 & F \end{bmatrix}, \quad B = \begin{bmatrix} B^0 \\ 0 \end{bmatrix}, \quad C = [C^0 \ 0], \quad (3)$$

together with

$$A^0 = \begin{bmatrix} 0 & 1 \\ -\mathcal{M}\beta_{r_0} & 0 \end{bmatrix}, \quad B^0 = \begin{bmatrix} 0 \\ \mathcal{M} \end{bmatrix}, \quad C^0 = [0 \ 1], \quad (4)$$

where $\beta_{r_0} \in \mathbb{R}^+$ is the so-called hydrostatic stiffness and $\mathcal{M} = (M + \mu_\infty)^{-1} \in \mathbb{R}^+$, with M the mass of the WEC

² From now on, the dependence on t is dropped when clear from the context.

³ See (Faedo et al., 2020b; Pérez and Fossen, 2008) for a formal discussion on the properties associated with Σ_r .

system, and μ_∞ the infinite frequency asymptote of the so-called radiation added-mass (see *e.g.* Korde and Ringwood (2016)).

The mapping $g : \mathbb{R}^n \rightarrow \mathbb{R}^n$, which is exclusively composed of terms characterising the nonlinear behaviour of system Σ in (1), can be written as

$$g(x) = \begin{bmatrix} g^0(x) \\ 0 \end{bmatrix}, \quad (5)$$

with g^0 defined as

$$g^0(x) = \begin{bmatrix} 0 \\ \mathcal{M}(-\alpha_v x_2 |x_2| + \beta_{r_1} x_1^2 + \beta_{r_2} x_1^3) \end{bmatrix}, \quad (6)$$

where the coefficient $\alpha_v \in \mathbb{R}^+$ represents nonlinear viscous effects, derived via the so-called Morison equation (see (Morison et al., 1950)), while the set $\{\beta_{r_1}, \beta_{r_2}\} \subset \mathbb{R}$ defines a polynomial representation of nonlinear restoring effects (see (Faedo et al., 2021a; Hals et al., 2016)).

3. OPTIMAL REFERENCE GENERATION

As discussed throughout Section 1, WEC energy-maximising control design procedures can be defined in terms of an associated OCP⁴, which essentially aims to maximise the energy absorbed from the wave field, *i.e.* the map

$$(u, y) \mapsto \int_{\Omega} \eta(u, y) uy \, d\tau, \quad (7)$$

with $\Omega = [0, T] \subset \mathbb{R}^+$, y the output of (1), and where $\eta : \mathbb{R} \times \mathbb{R} \rightarrow [0, 1]$, $(u, y) \mapsto \eta(u, y)$, denotes the so-called PTO efficiency map, describing the mechanical-to-electrical conversion stage efficiency. In particular, we consider, in this paper, the efficiency function explicitly used within the control benchmark case set by the Wave Energy Control Competition (WECCOMP) (see *e.g.* Ringwood et al. (2019)), *i.e.*

$$\eta(u, y) = \frac{\mu^2 - 1}{2\mu} \text{sign}(uy) + \frac{\mu^2 + 1}{2\mu}, \quad (8)$$

where $\mu \in [0, 1]$ is the so-called *efficiency factor* (which corresponds to the product of the average efficiencies of each potential PTO conversion stage). With the definition of the control objective in (7), and the PTO conversion efficiency map (8), the OCP can be formalised in terms of the following infinite-dimensional problem:

$$\begin{aligned} & \max_{(u, y)} \int_{\Omega} \eta(u, y) uy \, d\tau, \\ & \text{subject to:} \end{aligned} \quad (9)$$

$$\dot{x} = Ax + B\zeta + g(x), \quad y = Cx = x_2.$$

Within the particular control architecture exploited in this paper, given an external excitation force f_e , the objective is first to produce an optimal velocity reference $y^o \equiv \nu_{\text{ref}}$ via an appropriate solution of (9), to be tracked accordingly by the inner loop designed in Section 4. To achieve such an objective, we adopt the moment-based direct optimal control approach proposed by Faedo et al. (2021a), which transcribes the infinite-dimensional OCP (9) to a finite-dimensional nonlinear program. We briefly describe the steps towards computing such a moment-based solution in the following paragraph.

In line with the theoretical framework presented by Faedo et al. (2021a), we begin by assuming that $\{f_e, u\} \subset L^2(\Omega)$ and hence we adopt an implicit form representation for the maps of both f_e and u in (1) in terms of the following *signal generator*

$$\mathcal{G} : \begin{cases} \dot{\theta} = \underline{S}\theta, & f_e = \underline{L}_e\theta, & u = \underline{L}_u\theta, \end{cases} \quad (10)$$

with $\underline{S} \in \mathbb{R}^{\iota \times \iota}$, $\iota \in 2\mathbb{Z}/0$, such that $\lambda(\underline{S}) = \{j p \omega_0\}_{p=1}^{\iota/2} \subset \mathbb{C}^0$, and where the pair of matrices $(\underline{S}, \xi(0))$ is reachable. Given the nature of the state-transition map in (1), there exists (Faedo et al., 2021b) a unique mapping \mathcal{M} , locally defined in a neighbourhood Θ of the origin of (10), such that, for any fixed trajectory $\theta(t) \in \Theta$, the steady-state output response of system (1) driven by (10), is $y_{\text{ss}} = \mathcal{M}(\theta(t))$. Following (Faedo et al., 2021a), an approximation of the map \mathcal{M} , for a given trajectory $\theta(t)$, can be computed in terms of a finite-dimensional approximation over the space spanned by the set $\mathcal{F} = \{\theta_p\}_{p=1}^{\iota}$, *i.e.* $\mathcal{M}(\theta) \approx \underline{Y}\theta$, with $\underline{Y}^T \in \mathbb{R}^{\iota}$ computed via a Galerkin-like procedure, for any ι sufficiently large. In particular, the expansion coefficients \underline{Y} are obtained as the solution of an appropriate system of nonlinear equations

$$G(\underline{Y}, \underline{L}_u) = 0, \quad (11)$$

with the map $G : \mathbb{R}^{1 \times \iota} \rightarrow \mathbb{R}^{n \iota}$ obtained via orthogonal projection of a suitably defined residual function over \mathcal{F} , under the standard inner-product operation in $L^2(\Omega)$. With the definitions provided up until this point, we can approximate the OCP (9) in terms of the following NP

$$(\underline{Y}^o, \underline{L}_u^o) = \arg \max_{(\underline{Y}, \underline{L}_u)} \int_{\Omega} \eta(\underline{L}_u\theta, \underline{Y}\theta) \underline{L}_u\theta (\underline{Y}\theta)^T \, d\tau, \quad (12)$$

subject to:

$$G(\underline{Y}, \underline{L}_u) = 0,$$

where the optimal velocity reference can be computed from (12) as

$$y^o \equiv \nu_{\text{ref}} = \underline{Y}^o\theta. \quad (13)$$

Note that the algebraic constraint in (12), introduced in (11), ‘replaces’ the dynamical constraint in (9).

4. SOSM CONTROL DESIGN

In this section, we present a SOSM control design for optimal reference tracking. This type of control forces the state trajectories to evolve on a surface in the state space, which ensures control objective accomplishment. As mentioned in Section 1, SMC has certain properties that make it particularly interesting for uncertain systems, such as those arising from hydrodynamic modelling of WECs. Among their characteristics, can be highlighted: Finite time convergence to the designed surface in the state space, system order reduction, and robustness against certain disturbances. SOSM inherits most of these properties while acting on the second time derivative of the constraint function $\sigma(x)$, termed the sliding variable. SOSM works with a continuous action over $\dot{\sigma}(x)$, weakening the effect of chattering in the output, which provides greater accuracy. Additionally, in some applications (namely, plants with relative degree one with respect to σ), the resultant physical control input to the plant is continuous, contributing to longer service life of the actuators (Levant, 1993; Bartolini et al., 1999; Shtessel et al., 2013).

⁴ The reader is referred to Liberzon (2011) for a formal treatment of optimal control theory.

4.1 Sliding Variable Definition

The sliding surface in the phase-plane is reached when $\sigma = 0$. So, appropriate definition of the sliding variable facilitates control objective achievement. In this paper, the main objective is to maximise the wave energy capture of the device. We achieve this maximal energy capture by forcing the device to track the optimal velocity reference generation proposed in Section 3. Then, the sliding variable that will force robust tracking of the optimal reference is:

$$\sigma(x) = \nu_{\text{ref}} - x_2 \quad (14)$$

where ν_{ref} is the optimal velocity reference computed from (13) and x_2 is the state associated with the buoy velocity.

4.2 Objective Tracking Assurance

The sliding variable defined in (14) has relative degree one with respect to the control input, u . Mainly for this reason, the control algorithm selected here to accomplish the control objective is the Super-Twisting (ST) algorithm. This is one of the most widely used algorithms of the SOSM family, and it is particularly intended for systems with relative degree one (Hung et al., 1993; Fridman and Levant, 2002). Among the advantages mentioned earlier within this section, the ST algorithm synthesises a continuous control action and does not require the measurement of $\dot{\sigma}$ in the control law, which makes it more immune to output measurement noise.

The control law of the ST algorithm is composed of two continuous terms (Levant, 1993):

$$u(t) = -\beta|\sigma(t)|^{\frac{1}{2}}\text{sign}(\sigma(t)) - \alpha \int_0^t \text{sign}(\sigma(\tau))d\tau \quad (15)$$

where β and α are the control gains. The tuning of the Super-Twisting gains requires $\ddot{\sigma}$ to be expressed explicitly in terms of \dot{u} as

$$\ddot{\sigma} = \lambda(x, u) + \gamma(x)\dot{u}. \quad (16)$$

Consequently, differentiating σ twice:

$$\begin{aligned} \ddot{\sigma} = & \ddot{\nu}_{\text{ref}} + \mathcal{M}\beta_{r0}x_2 + H[Gx_2 + Fx_3] - \mathcal{M}\dot{f}_e + \\ & + \mathcal{M}(-\alpha_v|x_2|[\mathcal{M}\beta_{r0}x_1 + Hx_3 - \mathcal{M}(f_e - u) + \\ & + \mathcal{M}d_2(x)] + \beta_{r1}2x_1x_2 + \beta_{r2}x_1^2x_2) + \\ & + \mathcal{M}\dot{u} \end{aligned} \quad (17)$$

it can be determined that $\gamma = \mathcal{M}$, obtained from the last term of (17), and that $\lambda(x, u)$ covers the remaining terms. After this subdivision, (17) can be straightforwardly written as required in (16).

Then, to complete the ST controller design procedure, functions $\lambda(x, u)$ and γ must be bounded by means of three positive constants $\Gamma_m < \Gamma_M$ and C such that

$$|\lambda(x, u)| \leq C \quad (18)$$

$$\Gamma_m \leq \gamma \leq \Gamma_M,$$

taking into account disturbances and uncertainty bounds.

Finally, if the gains are selected so that they satisfy the sufficient conditions

$$\begin{aligned} \alpha &> \frac{C}{\Gamma_m} \\ \beta &> \frac{\sqrt{2(\alpha\Gamma_M + C)}}{\Gamma_m}, \end{aligned} \quad (19)$$

then, finite-time convergence to $\sigma = \dot{\sigma} = 0$ and robust SOSM operation are guaranteed, even in the presence of disturbances and uncertainties considered in the computation of the bounds.

5. NUMERICAL RESULTS

This section presents a numerical appraisal of the performance associated with the proposed SOSM strategy, for the device presented in Section 2. The specific values for the set of parameters describing (1) can be found in (Faedo et al., 2021a). The device is assumed to be excited by an irregular wave field, characterised by a JONSWAP spectral density function (Hasselmann et al., 1973), with significant wave height $H_s = 2$ m, peak period $T_p = 8$ s, and a peak-enhancement parameter of $\gamma = 3.3$. The excitation force, arising from the specific realisation considered for the evaluation of the controlled performance, is shown in Figure 3, and has a total time span of $T \approx 300$ s. The efficiency factor for the PTO system in equation (8) is set to $\mu = 0.8$, indicating 80% efficiency. Note that we assume full knowledge of f_e for the computation of the optimal velocity profile (13) within the set Ω , aiming to ‘decouple’ the estimation problem for the results presented within this section (Pena et al., 2020), which aims at assessing the performance of the proposed tracking controller.

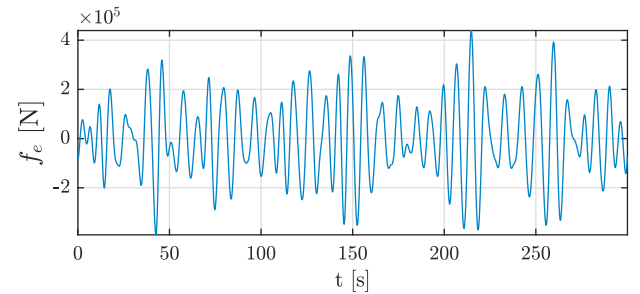


Fig. 3. Realisation of the excitation force utilised for presenting the results.

Also, with the objective to create a challenging scenario for the control tests, and demonstrate the robustness of the proposed controller, we add parameter uncertainty and perturbations that could appear in a typical WEC control implementation. For parameter uncertainty, we consider a 10% variation in the nominal mass of the device (possible due to biofouling), a 15% variation in hydrostatic stiffness β_{r0} and 20% uncertainty in the coefficients of the radiation state matrix, Γ (both by possible modelling errors). With these considerations, the ST controller gains are designed following Section 4.2, considering uncertainty and perturbations in the determination of the bounds in (18). After that, the values obtained using (19) were $\alpha = 1.5455 \times 10^6$ and $\beta = 1.0056 \times 10^6$.

Moreover, in this section, we provide a comparison of the performance of the designed SOSM controller against the most ubiquitous tracking control scheme, namely a Proportional-Integral (PI) controller, designed to execute the best possible tracking of the velocity reference. The gains we selected for this controller were $P = 3.0496 \times 10^6$ and $I = 4.5140 \times 10^6$.

The simulation starts with the device without the tracking control activated up to $t = 7.5$ s. Then, in a particular

simulation for each controller (SOSM and PI), we connect the control action in order to force the system to follow the designed velocity reference and to observe the velocity tracking performance when each controller is effectively acting on the WEC. The behaviour of the system with both controllers is shown in Fig. 4, where only the period up to 40 s is shown, to highlight the convergence of the velocity state to the reference and visualise, with greater detail, the robustness and disturbance rejection behaviour of each controller.

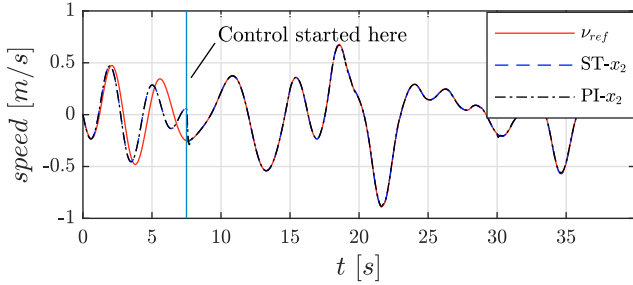


Fig. 4. Comparison between the ability to efficiently track the reference (in solid red) of the ST algorithm (dashed blue) and the PI controller (dot-dashed black).

When the system is governed by the SOSM controller, the trajectories converge in finite-time to the designed surface in the phase-plane. That finite-time convergence can be observed in Fig. 5. In this figure, the first 7.5 s part, corresponding to the period where no control action is applied to the buoy, can be observed using a dashed line. Then, when the control is activated, the system trajectory follows the characteristic convergence curve of the super-twisting controller, which reaches, in finite-time, the designed surface $\sigma = \dot{\sigma} = 0$, plotted using solid line.

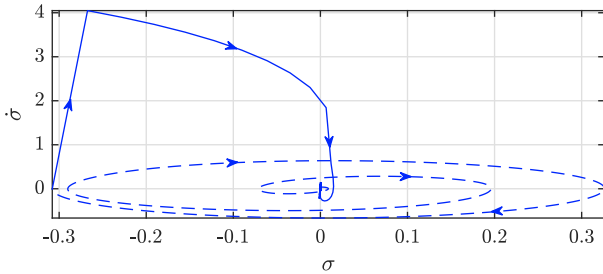


Fig. 5. Super-Twisting convergence in the phase plot $\sigma - \dot{\sigma}$. The dashed lines represent the movement of the system without control and the solid lines the system trajectories under SOSM control.

Further expanding the analysis of the proposed controller, we consider a perturbation that disturbs the system in terms of a sudden appearance of a force of the type $f_m = K_m x_1$, $K_m \in \mathbb{R}^+$. This force emulates a sudden safety restoring effect, potentially triggered by an extreme sea-state event, increasing system stiffness. This perturbation is set to affect the system at $t = 30$ s (see Fig. 6).

The finite-time convergence and reduced overshoot, compared with the PI controller, and robustness of the SOSM control technique (which, unlike the PI controller, can efficiently reject the perturbation), can be observed in Fig. 7.

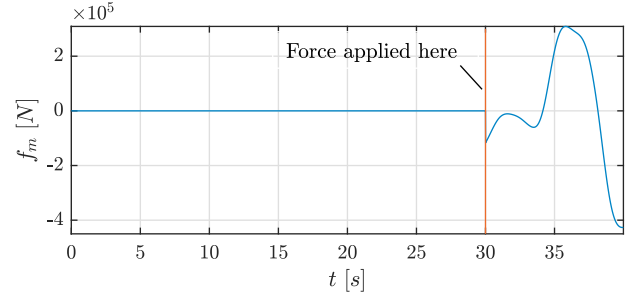


Fig. 6. Sudden appearance of a safety restoring force.

This figure plots the error ($\nu_{ref} - x_2$) when each controller is driving the buoy, with the ST controlled system error shown using a dashed blue line, and the PI controlled system error in dot-dashed black line. Axis *a*) shows the convergence of the controllers to the reference, where it is clear that the ST controller produces a lower overshoot, and reaches the reference in less time than the PI. On the other hand, subplots *b*) and *c*) show the response of each controller to the restoring force disturbance (f_m). Here, unlike the ST controller, it is evident that the PI strategy fails to keep the trajectories of the system at the reference when under the influence of the disturbance due to f_m .

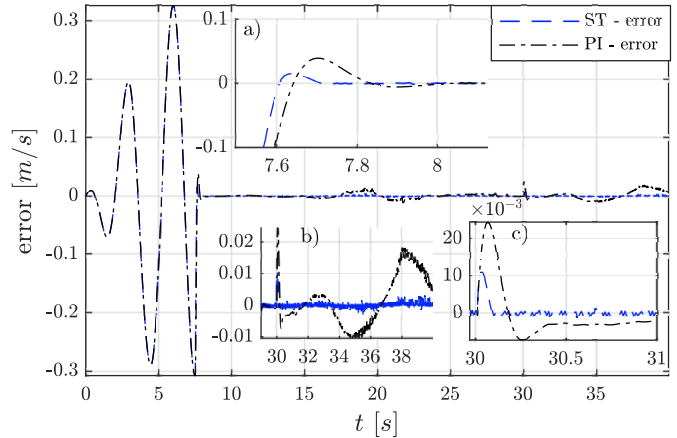


Fig. 7. Error in tracking the reference for both controllers. The error response with the ST controller is shown in dashed blue, while the response with the PI controller is black dash-dot.

6. CONCLUSIONS

Motivated by the inherent necessity of robust tracking control techniques to effectively achieve optimal performance in WEC systems, we design, in this paper, a second order sliding mode controller to robustly track an optimal energy-maximising velocity profile for a nonlinear point absorber WEC, computed via so-called moment-based theory. This is, to the best of our knowledge, the first application of SOSM control for a nonlinear heaving point absorber system.

The SOSM control technique proposed is a Super-Twisting algorithm, designed to intrinsically handle hydrodynamic parameter uncertainty, and sudden perturbations. The results presented in our paper show that the control technique efficiently deals with uncertainty, exhibiting a

significant robustness for each tested case, with finite time convergence to the optimal reference and mild computational requirements. Also, better tracking results are obtained when compared against a reference PI controller. Hence the ST is an ideal candidate for real-time energy-maximising control of WEC systems. Future work will assess the performance of the proposed controller in an experimental environment.

REFERENCES

- Bacelli, G. and Ringwood, J.V. (2014). Numerical optimal control of wave energy converters. *IEEE Transactions on Sustainable Energy*, 6(2), 294–302.
- Bartolini, G., Ferrara, A., Levant, A., and Usai, E. (1999). On second order sliding mode controllers. In *Var. Struct. Syst. Sliding Mode Nonlinear Control*, 329–350. Springer London, London.
- Faedo, N., García-Violini, D., Peña-Sánchez, Y., and Ringwood, J.V. (2020a). Optimisation-vs. non-optimisation-based energy-maximising control for wave energy converters: A case study. In *European Control Conference (ECC)*, 843–848. IEEE.
- Faedo, N., Olaya, S., and Ringwood, J.V. (2017). Optimal control, MPC and MPC-like algorithms for wave energy systems: An overview. *IFAC Journal of Systems and Control*, 1, 37–56.
- Faedo, N., Peña-Sánchez, Y., and Ringwood, J.V. (2020b). Parametric representation of arrays of wave energy converters for motion simulation and unknown input estimation: a moment-based approach. *Applied Ocean Research*, 98, 102055.
- Faedo, N., Scarciotti, G., Astolfi, A., and Ringwood, J.V. (2021a). Nonlinear energy-maximizing optimal control of wave energy systems: A moment-based approach. *IEEE Transactions on Control Systems Technology*, 29(6), 2533–2547.
- Faedo, N., Scarciotti, G., Astolfi, A., and Ringwood, J.V. (2021b). On the approximation of moments for nonlinear systems. *IEEE Transactions on Automatic Control*, 66(11), 5538–5545.
- Fridman, L. and Levant, A. (2002). Higher-Order Sliding Modes. In *Sliding Mode Control Eng.*, chapter 3, 53–101. CRC Press.
- Genest, R. and Ringwood, J.V. (2016). Receding horizon pseudospectral control for energy maximization with application to wave energy devices. *IEEE Transactions on Control Systems Technology*, 25(1), 29–38.
- Giorgi, G., Gomes, R.P., Henriques, J.C., Gato, L.M., Bracco, G., and Mattiazzo, G. (2020). Detecting parametric resonance in a floating oscillating water column device for wave energy conversion: Numerical simulations and validation with physical model tests. *Applied Energy*, 276, 115421.
- Hals, J., Ásgeirsson, G.S., Hjalmarsson, E., Maillet, J., Möller, P., Pires, P., Guérinel, M., and Lopes, M. (2016). Tank testing of an inherently phase-controlled wave energy converter. *Int. J. of Marine Energy*, 15, 68–84.
- Hals, J., Falnes, J., and Moan, T. (2011). Constrained optimal control of a heaving buoy wave-energy converter. *Journal of Offshore Mech. and Arctic Eng.*, 133(1).
- Hasselmann, K.F., Barnett, T.P., Bouws, E., Carlson, H., Cartwright, D.E., Eake, K., Euring, J., Gignapp, A., Hasselmann, D., Kruseman, P., et al. (1973). Measurements of wind-wave growth and swell decay during the joint north sea wave project (JONSWAP). *Ergänzungsheft zur Deutschen Hydrographischen Zeitschrift*.
- Herber, D.R. and Allison, J.T. (2013). Wave energy extraction maximization in irregular ocean waves using pseudospectral methods. In *International Design Engineering Technical Conferences and Computers and Information in Engineering Conference*, volume 3. American Society of Mechanical Engineers.
- Hung, J.Y., Gao, W., and Hung, J.C. (1993). Variable structure control: a survey. *IEEE Trans. Ind. Electron.*, 40(1), 2–22.
- Korde, U.A. and Ringwood, J.V. (2016). *Hydrodynamic Control of Wave Energy Devices*. Cambridge U. Press.
- Levant, A. (1993). Sliding order and sliding accuracy in sliding mode control. *Int. J. Control*, 58(6), 1247–1263.
- Li, G. (2017). Nonlinear model predictive control of a wave energy converter based on differential flatness parameterisation. *Int. J. Control*, 90(1), 68–77.
- Liberzon, D. (2011). *Calculus of Variations and Optimal Control Theory*. Princeton University Press.
- Morison, J., Johnson, J., Schaaf, S., et al. (1950). The force exerted by surface waves on piles. *Journal of Petroleum Technology*, 2(05), 149–154.
- Pena, Y., Windt, C., Davidson, J., and Ringwood, J. (2020). A critical comparison of excitation force estimators for wave energy devices. *IEEE Trans. on Control Systems Technology*, 28, 2263–2275.
- Pérez, T. and Fossen, T.I. (2008). Time-vs. frequency-domain identification of parametric radiation force models for marine structures at zero speed. *Modeling, Identification and Control*, 29(1), 1–19.
- Ringwood, J., Ferri, F., Tom, N., Ruehl, K., Faedo, N., Bacelli, G., Yu, Y.H., and Coe, R.G. (2019). The wave energy converter control competition: Overview. In *Int. Conf. on Offshore Mechanics and Arctic Engineering*. American Society of Mechanical Engineers.
- Ringwood, J.V. (2020). Wave energy control: status and perspectives 2020. *IFAC-PapersOnLine*, 53(2), 12271–12282.
- Ringwood, J.V. and Simani, S. (2015). Overview of modelling and control strategies for wind turbines and wave energy devices: Comparisons and contrasts. *Annual Reviews in Control*, 40, 27–49.
- Shtessel, Y., Edwards, C., Fridman, L., and Levant, A. (2013). *Sliding Mode Control and Observation*. Springer New York.
- Utkin, V.I. and Lee, H. (2006). Chattering problem in sliding mode control systems. In *International Workshop on Variable Structure Systems, 2006. VSS'06.*, 346–350.
- Wahyudie, A., Jama, M.A., Assi, A., and Noura, H. (2013). Sliding mode and fuzzy logic control for heaving wave energy converter. In *52nd IEEE Conference on Decision and Control*, 1671–1677.
- Zhang, Y. and Li, G. (2020). Non-causal linear optimal control of wave energy converters with enhanced robustness by sliding mode control. *IEEE Transactions on Sustainable Energy*, 11(4), 2201–2209.